Food and Chemical Toxicology 127 (2019) 11–18

Contents lists available at ScienceDirect

Food and Chemical Toxicology

journal homepage: www.elsevier.com/locate/foodchemtox

Lutein derived from marigold (*Tagetes erecta*) petals triggers ROS generation and activates Bax and caspase-3 mediated apoptosis of human cervical carcinoma (HeLa) cells

Enkhtaivan Gansukh[a], Khine Khine Mya[a,c], Mina Jung[a], Young-Soo Keum[c], Doo Hwan Kim[a], Ramesh Kumar Saini[a,b,c,*]

[a] Department of Bioresources and Food Science, Konkuk University, Seoul 143-701, Republic of Korea
[b] Institute of Natural Science and Agriculture, Konkuk University, Seoul 143-701, Republic of Korea
[c] Department of Crop Science, Konkuk University, Seoul 143-701, Republic of Korea

ARTICLE INFO

Keywords:
Carotenoids
Oxidative stress-mediated apoptosis
Mitochondrial membrane potential
TUNEL assay
DNA fragmentation

ABSTRACT

The present investigation was designed to determine molecular and cellular events involved in anticancer properties of lutein derived from marigold (*Tagetes erecta*) petals using Human cervical carcinoma (HeLa) cell lines. *In vitro* experiments demonstrated that lutein at concentration of 10 μM significantly inhibited proliferation of HeLa cells by up to 62.85% after 24 h of treatment and 84.85% after 48 h of treatment. In addition, lutein inhibited proliferation of HeLa cells in a dose-dependent manner by inducing apoptosis. Lutein-treated HeLa cells also showed enhanced accumulation of reactive oxygen species (ROS) correlated with significant down-regulation of Bcl-2 (anti-apoptotic) expression and upregulation of Bax (pro-apoptotic) expression. Furthermore, lutein mediated activation of caspase-3 and imbalance between Bax and Bcl-2 expression, causing significant loss of mitochondrial membrane potential of HeLa cells. TUNEL assays revealed significant damage of nuclei DNA in lutein-treated HeLa cells, demonstrating a critical role of lutein in the final stage of apoptosis. Taken together, the results indicate that lutein-induced apoptosis of HeLa cells occurs through enhanced ROS production, interaction with mitochondrial factors, and upregulation of caspase-3-mediated pathway, leading to fragmentation of nuclei DNA. Therefore, lutein could be potentially useful as a chemotherapeutic and/or chemopreventive biomolecule against Human cervical carcinoma.

1. Introduction

Dietary consumption of fruits, flowers, vegetables, and microalgae that are rich in carotenoids is associated with lower risk for several types of cancer, age-related macular degeneration (AMD), and cardiovascular diseases (CVD) (Lakshminarayana et al., 2010). To date, nearly 700 carotenoids have been identified (Nupur et al., 2016). Based on the presence of oxygenated functional groups, these carotenoids are generally classified into two major classes: i) hydrocarbon carotenoids that are referred to as carotenes (either linear or cyclized such as lycopene, α-carotene, and β-carotene); and ii) oxygenated derivatives of carotenes that are known as xanthophylls (e.g., Neoxanthin, lutein, zeaxanthin, β-cryptoxanthin, and astaxanthin). Lutein (β,ε-carotene-3,3-diol) is one of the most widely occurring xanthophyll carotenoids in the plant kingdom. In nature, flower petals of yellow Marigold (*Tagetes erecta* L.) are considered the most abundant source of lutein (Nwachukwu et al., 2016). Dietary consumption of lutein is generally recognized as safe (GRAS) without adverse effects following long-term dietary supplementation with 30–40 mg/day (Nwachukwu et al., 2016).

The characteristic yellow-red color of lutein and its β-isomer zeaxanthin (β,β-carotene-3,3′-diol) is attributed to the presence of a polyene chain $(-C=C-)_n$ with ten conjugated carbon-carbon double bonds (11 in case of zeaxanthin) that function as a chromophore (Widomska and Subczynski, 2014). Moreover, the high reducing potential of its polyene chain provides effective neutralization of ROS by physical quenching

Abbreviations: AMD, Age-related macular degeneration; Bax, Bcl-2-associated X protein; Bcl, B-cell lymphoma; CVD, Cardiovascular diseases; GRAS, Generally recognized as safe; HDI, Human development index; HeLa, Human cervical carcinoma; HPLC, High performance liquid chromatography; MDCK, Madin-Darby Canine Kidney; PBS, Phosphate buffered solution; ROS, Reactive oxygen species; SRB, Sulforhodamine B; TUNEL, Terminal deoxynucleotidyl transferase-mediated dUTP nick end labeling

* Corresponding author. Department of Bioresources and Food Science, Konkuk University, Seoul 143-701, Republic of Korea.
E-mail address: saini1997@konkuk.ac.kr (R.K. Saini).

https://doi.org/10.1016/j.fct.2019.02.037
Received 29 October 2018; Received in revised form 15 February 2019; Accepted 25 February 2019
Available online 01 March 2019
0278-6915/

(deactivation of singlet oxygen to the nonreactive triplet state) and chemical quenching (carotenoids autoxidation) (Widomska and Subczynski, 2014). Among several carotenoids found in the animal body, lutein and zeaxanthin can selectively accumulate in lipid membranes of the retina to provide protection against oxidative stress, neutralize photosensitizers, and ROS (Widomska and Subczynski, 2014). Minimum daily consumption of 2.4 mg lutein/day and 1.3 mg zeaxanthin/day is recommended to minimize the risk of age-related macular degeneration (Alvarado-Ramos et al., 2018). However, low dietary intake of 0.9–1.7 mg/day of lutein and 0.5–0.6 mg/day of zeaxanthin has been recorded among different studies (Alvarado-Ramos et al., 2018). Fruits and vegetable principally contribute to dietary intake of lutein and zeaxanthin whereas carotenoid supplements rarely contribute to it (Alvarado-Ramos et al., 2018).

Cancer is the second leading cause of death globally and is responsible for an estimated 9.6 million deaths in 2018. In recent years, cancer diseases are growing tremendously due to environmental pollution and unhealthy lifestyles. Based on recent statistical reports, 15.7% of human deaths (8.8 million) were caused by cancer in 2015, excluding skin cancer (Wang et al., 2016). Expenses of diagnosis and treatment for cancer might be too expensive to be covered by ordinary family income. Worldwide, cervical cancer is the 4th most common cause of cancer in women (Bernard, 2014). In the Year 2012, 368,000 cases of cervical cancer were recorded with 199,000 deaths (Bernard, 2014). About 70% of cases of cervical cancers occurs in countries with low/medium human development index (HDI). Widespread use of cervical screening program has adequately reduced occurring rates of cervical cancer in low/medium HDI countries (Canavan and Doshi, 2000). In medical science, human cervical carcinoma (HeLa) cell line is the most influential cell line. It was originally isolated from cervical cancer cells of a woman named Henrietta Lacks (Carraher, 2013). This cell line has facilitated many cancer-related scientific researches to improve our understanding of cancer and obtain cheaper and more effective drugs which has become the highest priority.

To elucidate the antitumor activity of natural carotenoids, both *in vitro* and *in vivo* models have been used in research studies in the past three decades (Niranjana et al., 2015). However, most of these previous *in vitro* studies on natural carotenoids have been conducted on carcinoma derived from prostate (PC-3) (Kotake-Nara et al., 2005, 2001), breast (MCF-7) (Sowmya et al., 2017; Vijay et al., 2018), and blood-forming (HL-60) cells (Ganesan et al., 2011; Kim et al., 2010). The present study is the first systematic study on lutein-mediated regulation of the accumulation of cellular ROS, interaction with mitochondrial factors, expression of anti-apoptotic (Bcl-2; B-cell lymphoma-2) and pro-apoptotic [Bcl-2-associated X protein (Bax), tumor protein p53 (p53) and caspase-3] proteins in HeLa cells and normal MDCK cells. Additionally, the impact of lutein treatment on mitochondrial membrane potential and the integrity of nuclei DNA was investigated in this study.

2. Material and methods

2.1. Plant material, cell culture reagents, and standards

Plants of the Mexican marigold (*Tagetes erecta*) were cultivated in a commercial farm located in Paju city in Gyeonggi Province, South Korea from March to August 2018. These plants were cultivated following natural farming practices without using any chemical herbicide, pesticides, or fertilizers. The plant species (*T. erecta*) was authenticated by a floriculture specialist of Institute of Natural Science and Agriculture, Konkuk University. The harvesting of fully opened flowers (~3 kg) was manually carried out early in the morning on a single occasion (July 2018). These flowers were brought to the laboratory, petals were separated, oven dried at 50 °C for 24 h, ground in a food processor, sieved through a 500 μm sieve, and stored at −80 °C in an ultra-low temperature deep freezer.

Human cervical carcinoma cells (HeLa cells) and Madin-Darby Canine Kidney (MDCK) cells were obtained from American Type Tissue Culture Collection (CCL-34, ATCC, USA). They were maintained with Dulbecco's Modified Eagle's Medium (DMEM, Gibco BRL, Grand Island, NY, USA) supplemented with 0.01% of penicillin (Gibco BRL, Grand Island, NY, USA) and 10% of fetal bovine serum (FBS, Gibco BRL, Grand Island, NY, USA) in a humidified incubator at 37 °C with 5% CO_2.

2.2. Green extraction of lutein

In the first step, extraction efficiencies of two green solvents (cyclohexane and n-heptane) were compared with those of conventionally and widely used solvent n-hexane for efficient extraction lutein from marigold petals. Carotenoids were separately extracted by solid-liquid extraction with n-hexane, cyclohexane, and n-heptane. Key steps used in the extraction were based on findings from Rodriguez-Amaya (2001). All the experimental preparations of extraction and purification were conducted in dim or yellow light to avoid light-induced degradation. Briefly, 1 g of marigold petals powder was transferred into a conical flask containing 50 ml of extraction solvent. Samples were homogenized with a mechanical homogenizer (HG-15A, Daihan Scientific Co. Ltd., Seoul, Korea) followed by centrifugation at 5000 × *g* for 5 min at 4 °C and the supernatant was then recovered. The pellet sample was repeatedly extracted until obtaining white pellets. Collected supernatants were pooled (~150 ml) and vacuumed evaporated in a rotary evaporator (Büchi RE 111, Switzerland) at temperature < 35 °C to obtain oleoresin extract. The obtained oleoresin was recovered in 15 ml of respective extraction solvent. Lutein content was then determined using a UV–Vis spectrophotometer as described in section 2.4 (HPLC, mass spectrometric (MS) and spectrophotometric analysis of isolated lutein). Lutein yield obtained by using green solvent n-heptane was comparable to that using n-hexane (Appendix 1, Supplementary material). Thus, for further experiments of lutein purification, oleoresin was extracted from 10 g dehydrated marigold powder using n-heptane. All organic solvents used for extraction of lutein were of HPLC grade obtained from Daejung Chemicals & Metals Co., Ltd., Korea.

For saponification, oleoresin obtained from using n-heptane for extraction was recovered in 100 ml of n-heptane and added to 250 ml volumetric flask. It was then mixed with 100 ml of 10% ethanolic-potassium hydroxide (KOH). Tubes were flushed with nitrogen gas (N2) and incubated at 55 °C for 20 min. After that, lipophilic fraction was recovered by repeated partitioning (3x) with respective exaction solvent using a separating funnel. Residues of KOH were removed by repeated (n = 3) water wash. Recovered solvents were pooled and vacuumed evaporated in a rotary evaporator (temperature < 35 °C). The dried saponified oleoresin extract was recovered in 100 ml ethanol and stored at −20 °C until preparative thin layer chromatography (TLC) purification of lutein.

2.3. Purification of lutein from saponified oleoresin

Preparative TLC was performed to purify lutein using Silica Gel GF plates (20 × 20 cm, 1500μ layer from Analtech Inc). The TLC plates were developed in glass tanks lined with filter paper and equilibrated with ~200 ml of acetone/hexane mixture (1:1) for 20 min before development. Approximately 200 μl of saponified ethanol extract was applied as a continuous line to the TLC plate with the help of 1.5 mm glass capillaries (Marienfeld, Lauda-Konigshofen, Germany) (Saini et al., 2018). Chromatograms were developed till the end of the plate (~45 min) at ambient temperature. The most dominant band of lutein found at Rf value of 0.76 was scrapped and added to the conical flask. A total of 10 plated were developed and lutein bands were scrapped. From the scrapped matrix, lutein was recovered by thoroughly mixing with acetone followed by centrifugation at 10,000 × *g* for 5 min. Collected supernatants were pooled and lutein content was measured spectrophotometrically, evaporated to dryness under a stream of

nitrogen, flushed with nitrogen gas (N2), and stored at −20 °C, until further spectrophotometric, HPLC, mass spectrometric analysis, and cell culture studies.

2.4. HPLC, mass spectrometric (MS), and spectrophotometric analysis of isolated lutein

Contents of the isolated lutein fraction were determined using a UV–Vis spectrophotometer (Shimadzu, Japan, Model UV-2550). For spectrophotometric quantification, 1 ml of the crude extract or purified lutein sample was filtered using a 0.45 μm Nylon syringe filter (Whatman Inc., USA) and diluted in ethanol. The absorbance was then recorded at a wavelength of 445 nm. The concentration of lutein was calculated using specific absorption coefficient (A1cm, 1%) of 2550 at 445 nm (in ethanol) (Hurst, 2008).

High-performance liquid chromatography (HPLC) was used to determine the % purity of purified lutein. For HPLC analysis, 1 ml of purified lutein (in acetone or ethanol) was filtered using a 0.45 μm Nylon syringe filter (Whatman Inc., USA) and transferred to an amber color HPLC vial. Chromatographic separation of purified lutein fractions were achieved using an Agilent Model 1100 HPLC instrument (Agilent Technologies Inc., Mississauga, Canada) equipped with a diode array detector (DAD), and a YMC C-30 carotenoid column (250 × 4.6 mm, 5 μm; YMC/Waters Inc., Wilmington, USA), maintained at 20 °C in a column thermostat. The optimized HPLC parameters were as follows: samples scanning wavelengths, 200–800 nm; response time, 1 s; slit width, 8 mm; detection wavelength, 450 nm with ± 16 nm bandwidth; reference wavelength; 600 nm with ± 50 nm bandwidth; injection volume, 20 μl. The mobile phases consisted of methanol/water (95:5) (mobile phase A) containing 5 mM ammonium formate, and tert-butyl methyl ether/methanol (91:9) (Mobile phase B). A gradient elution was followed form 0% B to 100% B for a total of 45 min analysis time, with a constant flow rate of 1 ml/min. Then a 5-min post run was kept (Kim et al., 2018). Ammonium formate was used to enhance ionization during mass spectrometric analysis.

Mass Spectrometry (MS) and Tandem mass spectrometry (MS/MS or MS2) analyses were conducted on a SCIEX API 3200™ triple quadrupole mass spectrometer (Applied Biosystems/MDS SCIEX, Foster City, CA, USA) equipped with an Exion LC™ system. To obtain Q1 mass spectrum, LC-separation was performed using the above described HPLC conditions. For MS/MS analysis, purified lutein fractions were dissolved in HPLC Mobile phase and data were acquired by direct infusion for 1 min at a flow rate of 10 μL/min using multiple-channel acquisition (MCA). All mass spectrometry experiments were performed in positive ion mode with atmospheric-pressure chemical ionization $(APCI)^+$. Other optimized MS and MS/MS parameters were as follows: temperature, 400 °C; dry gas, N2; curtain gas (CUR), 30 psi; collision gas (CAD) 5 psi; nebulizer current, 4 nA; ion source gas (GAS1), 45 psi; ion source gas (GAS2), 5 psi; delustering potential (DP), 100 V; entrance potential (EP), 10; collision energy (CE), 40 V; collision cell exit potential (CXP), 7 V (CXP start) to 28 V (CXP stop); and collision cell entrance potential (CEP), 7 V (CEP start) to 25 V (CXP stop). Q1 and MS/MS mass spectrum were acquired with a scan time of 1 s and a scan range from m/z 100 to 700.

2.5. Anticancer activities of purified lutein: sulforhodamine B (SRB) assay

Cytotoxicity assay was performed according to our previously established protocol (Saini et al., 2018) with minor modifications. Key steps of the adopted protocol were originally based on findings from Vichai and Kirtikara (2006). Briefly, HeLa or MDCK cells (1.5×10^5/ml) were seeded into 96-well plates and incubated at 37 °C for 12 h in a cell culture incubator with 5% CO_2. The medium was removed and plates were washed with 1x phosphate buffered solution (PBS). Cells were treated with lutein at final concentration of 50, 10, 1, and 0.1 μM (in triplicates) and incubated for 48 h. After removing the medium, plate was washed with 1xPBS. Cells were then fixed with 70% of cold acetone for 30 min at −4 °C and immediately dried in an oven at 60 °C. After fixing, SRB dye (0.4% w/v in 1% acetic acid) was used to determine the anticancer and cytotoxic effects of lutein. After 100 μL of SRB solution was added into each well, the plate was incubated at room temperature overnight on a rocket shaker. The next day, dye solution was then removed from plates. Plates were then washed five times with 1% acetic acid to remove unbounded SRB dyes. Washed plates were thoroughly dried in an oven at 60 °C for morphological observation using a reflected light microscope (AxioVert200 Carl Zeiss, Germany). Images were captured with AxioVision software (Carl Zeiss, Germany).

2.6. RNA isolation and qPCR

Total cellular RNA was isolated from cells using TRIZOL reagent (Invitrogen, USA) following the manufacturer's protocol. The isolated total RNA was reverse transcribed to cDNA using the First Strand cDNA Synthesis Kit (Thermo Fisher Scientific, Synthesis Kit (Thermo Fisher Scientific, Inc., Middletown, USA) following the manufacturer's instructions. The quantitative real-time PCR (qPCR) analysis was performed using gene-specific primers (Appendix 2, Supplementary material) and SYBR Green Master Mix (Bioneer, USA) followed the manufacturer's instructions. Expression levels of specific genes were normalized against the expression of glyceraldehyde-3-phosphate dehydrogenase (GAPDH) gene. Relative gene expression was calculated according to the $2^{-\Delta\Delta CT}$ method (Gansukh et al., 2016).

2.7. ROS production assay

ROS production was estimated following a previously established method (Gansukh et al., 2016). Briefly, HeLa or MDCK cells (2×10^4 cells/well) were cultured in 6-well plates and maintained for 24 h. Overproduction of ROS was stimulated by treatment with H_2O_2 (250 μM). ROS stimulated or non-stimulated cells were then treated with lutein (1 and 10 μM) for 24 h. Cell membrane-permeable isomeric mixture of fluorescent probe 5-(and-6)-carboxy-2′,7′-dichlorofluorescein diacetate (carboxy-H_2DCFDA, Sigma Aldrich) was used to monitor cellular ROS production. Cells were incubated with 10 μM of carboxy-H_2DCFDA at 37 °C for 15 min in a cell culture incubator and then washed three times with PBS. The intensity of ROS level was obtained using a fluorescent microplate reader (Molecular Devices, SpectraMAX Gemini EM). Values are expressed as relative fluorescent units.

2.8. Immunofluorescence assay for caspase-3 and mitochondrial membrane potential

HeLa cells were cultured on confocal dish at density of 2×10^4 cells/well and then treated with lutein (1 and 10 μM) for 24 h. At the end of treatment, cells in the lower wells were taken and washed with PBS (Pandurangan et al., 2016). Cells were fixed with 4% of paraformaldehyde for 15 min followed by permeabilization with 0.1% Triton X-100 in PBS for 20 min. They were finally rinsed twice with ice-cold PBS. The cells were blocked with 3% bovine serum albumin (BSA, w/v) for 30 min and incubated with cleaved Caspase-3 (Asp175) antibody (catalog # 9661; Cell signaling technology, Danvers, MA) for 3 h at 4 °C in 1% of BSA. After washing 5 times with PBS, cells were incubated with fluorescein isothiocyanate (FITC)-conjugated donkey anti-rabbit IgG (H and L) secondary antibody and then washed twice in PBS. Additionally, mitoRed for mitochondrial membrane permeability (Santa Cruz Biotechnology, South Korea) and DAPI for nuclei (Santa Cruz Biotechnology, South Korea) were used in the same experiment. These confocal dishes were mounted with a fluorescent mounting medium and observed under a Confocal Laser Scanning Microscope (Zeiss LSM-800, Carl Zeiss). Images were captured with Zen-Black Edition software (Zen 2.3 SP1, Version: 14.0, Carl Zeiss).

2.9. TUNEL assay

Terminal deoxynucleotidyl transferase-mediated dUTP nick end labeling (TUNEL) assay (Click-iT TUNEL Alexa Fluor 647, Life Technologies, USA) was carried out according to the manufacturer's protocol. Briefly, cells were seeded onto glass-bottom confocal culture dishes (SPL Life Sciences Co., Ltd. USA) at density of 1×10^5 cells/ml. After 24 h of adherence, cells were washed and treated with or without lutein at concentration of 1.0 μM or 10.0 μM for 24 h. Cells were fixed with 4% formaldehyde for 20 min and then permeabilized with 0.25% Triton X-100 for 25 min. Click-iT and TdT reactions were carried out according to kit instruction. TUNEL image was taken using an Olympus FLUOVIEW FV1200 confocal microscope (40 ×) (Olympus Corporation, Tokyo, Japan).

2.10. Statistical analyses

Values represent the mean ± SD of three independent replicates. Results of biological and analytical assay replicates were analyzed using ANOVA (IBM SPSS Statistics 22, SPSS Inc., Chicago, IL, USA). Tukey's test at $p < 0.05$ was employed to determine significant differences between treatments.

3. Result and discussion

3.1. Extraction, purification, and characterization of lutein

In the present study, lutein (β,ε-carotene-3,3-diol) was successfully purified with a high purity of 92.2% using a simple one-step preparative TLC (Fig. 1a and b). Following guidelines of Rodriguez-Amaya (2001), a combination of several parameters were used to accurately identify lutein, including the following: i) chromatographic properties in TLC (Rf) and HPLC (retention time) (Fig. 1A); ii) absorption spectrum (λ_{max} and fine structure) (Fig. 1B and C); and iii) mass spectrum (Fig. 1D and E). Visible spectra (λ_{max} of 444 and 472 nm) recorded during HPLC analysis in mobile phase by DAD detector, spectral fine structures (% III/II of 50), APCI$^+$-Q1 mass spectrum of m/z 569.3, and fragmentation pattern (Fig. 1E) of lutein molecule confirmed the identity of purified (all-*E*)-lutein (Saini et al., 2018). A unique ion fragment at 495 m/z was produced by the loss of hydroxyl (−OH) group of the protonated molecule and retro-Diels-Alder fragmentation of (all-*E*)-lutein $[MH–18–56]^+$ (Fig. 1D and E). Similarly, a low abundance ion fragment at 429.3 m/z was probably formed by elimination of the terminal α-ring from the non-conjugated carbon-carbon bond of (all-*E*)-lutein (Fig. 1D) (van Breemen et al., 2012). Characteristic positive ions at m/z 551.4 $[M + H–H_2O]^+$ and 533.3 $[M + H–2H_2O]^+$ further confirmed the identity of purified (all-*E*)-lutein (Saini et al., 2018). In the present study, ~200 μg of lutein was purified from a single 20 × 20 cm TLC plate. Moreover, a total of ~1800 μg of lutein was isolated from 10 plates which was found adequate to perform *in vitro* anticancer studies.

Despite concerns of environmental (air, water, and persistence), health (chronic and acute toxicity and irritation), safety (decomposition, explosion) issues and residual solvents in the product, carotenoids extraction by means of toxic organic solvent is still a common practice (Nwachukwu et al., 2016). Usually, a non-polar solvent such as n-hexane is an excellent choice for extraction of marigold oleoresin containing esterified lutein (Hojnik et al., 2008; Vechpanich and Shotipruk, 2010). Based on environmental, health, and legislation flag (regulatory restrictions), cyclohexane and n-heptane are preferred solvents compared to hexane (Henderson et al., 2011). In the present study, relative extraction efficiencies of hexane, cyclohexane, and n-heptane were compared for the extraction of lutein oleoresin. Results showed that n-heptane and n-hexane were equally efficient in extracting lutein. They had higher yields of lutein (12.48 and 12.28 mg/DW, respectively) than cyclohexane extraction (11.64 mg/DW) (Appendix 1, Supplementary material). These results provide vital evidence to possibly replace the use of toxic n-hexane with greener solvents such as n-heptane for the extraction of lutein from dehydrated

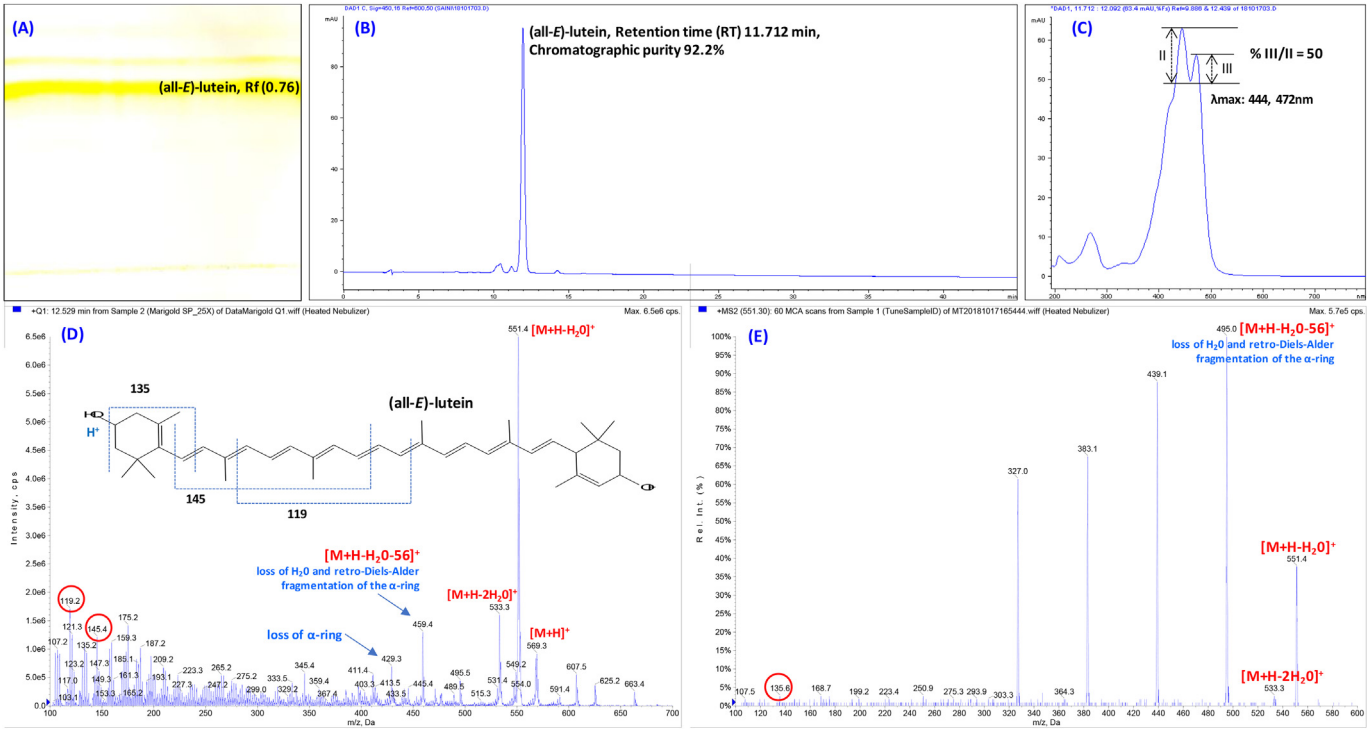

Fig. 1. Extraction, purification, and characterization of lutein. Silica Gel GF TLC plates showing clear separation of lutein (A), a major carotenoids of marigold oleoresin. HPLC-PDA chromatogram of purified lutein at 450 nm (B), showing high chromatographic purity. UV–visible spectra (λ_{max}) of lutein recorded during HPLC analysis in mobile phase by PDA detector (C). The Q1 mass spectrum of purified lutein recorded in APCI positive mode (D), and the tandem mass spectrum (MS/MS) of lutein molecule showing major fragments of m/z 551.2 $[M + H\text{-}H_20]^+$ (E).

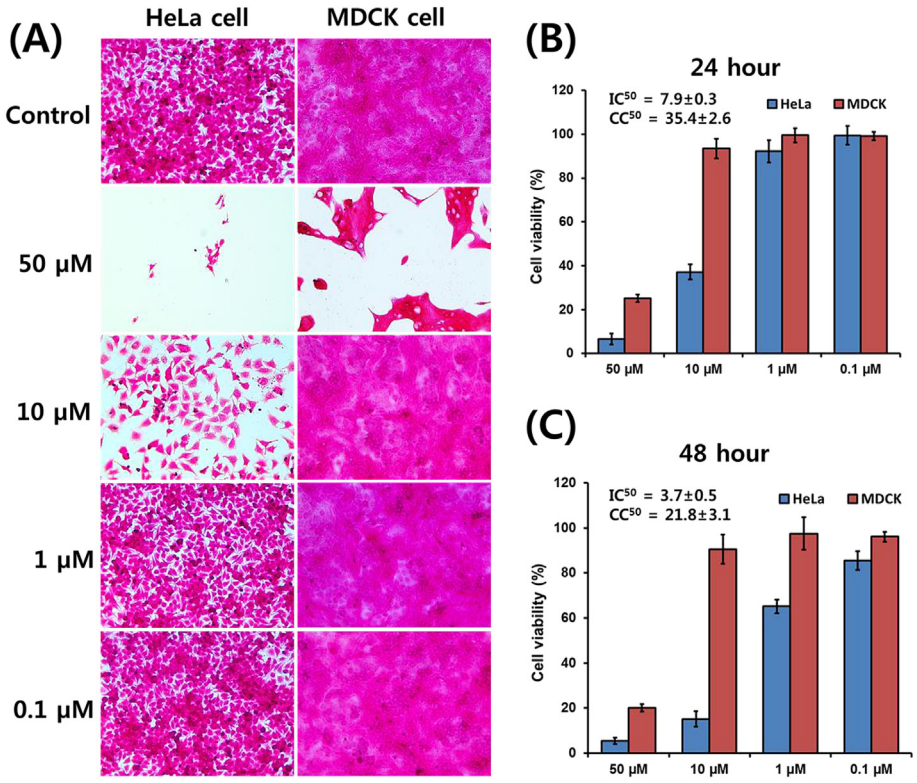

Fig. 2. Effects of lutein treatment on proliferation of HeLa and MDCK cells. Different concentrations (0.1–50 μM) of lutein were used to treat HeLa and MDCK cells. The morphology of cells (24 h of incubation) was documented using a light microscope with SRB assay (A). Cell viability after 24 h (B) and 48 h (C) of incubation. IC50: 50% inhibition concentration of HeLa cell, CC50: 50% cytotoxic concentration of MDCK cell. Error bars indicate standard deviation of three independent experiments.

marigold pastels.

3.2. Inhibitory effect of lutein on growth of HeLa cells

To determine anticancer and cytotoxic effect of lutein (0.1–50 μM) on normal (MDCK) and cervical tumor (HeLa) cells, SRB assays were performed. Results showed that lutein treatment at concentration of 10 μM was highly cytotoxic to cancer cells. It inhibited growth of HeLa cells by up to 62.85% and 84.85% after 24 h and 48 h of incubation, respectively. Also, lutein inhibited proliferation of HeLa cells in a dose-dependent manner (Fig. 2). On the other hand, lutein treatment (10 μM) did not have significant effect on the growth of MDCK cells after 24 h or 48 h of incubation. Interestingly, continuous incubation with lutein was found to be safe for normal cells. Previous studies have shown that lutein at concentrations of 5–20 μM can significantly inhibit the proliferation of various cell lines, including cervical cancer cells (HeLa), prostate cancer cells (PC-3, DU 145, and LNCaP), MCF-7 mammary carcinoma cells, SV40 transformed mammary cells, and oral cancer (KB-1) cells (Kotake-Nara et al., 2001; Krinsky and Johnson, 2005; Niranjana et al., 2015; Saini et al., 2018). It has also been reported that treatment with xanthophyll at concentration up to 100 μM is less toxic to normal cells than that to cancer cells (Saini et al., 2018).

3.3. Lutein triggers ROS generation and induced apoptosis of HeLa cells

ROS, including hydroxyl radical ($^{\cdot}OH$), singlet oxygen ($^1\Delta_g$), nitrogen dioxide ($^{\cdot}NO_2$), nitric oxide ($^{\cdot}NO$), superoxide ($^{\cdot}O_2^-$), and lipid peroxyl play a crucial role in the development of chronic degenerative diseases such as cancer, AMD, CVD, and neurodegenerative diseases (Pham-Huy et al., 2008). Cellular ROS is produced and eliminated in the living system to maintain regulatory metabolism (Pandurangan et al., 2016). Normal cells can manage ROS level by free radical scavenging system under normal level (Enkhtaivan et al., 2017). Cancer cells generate higher ROS levels than normal cells for their increased metabolic activity, mitochondrial malfunction, and oncogenic stimulation. Excessive ROS generation can damage DNA, proteins, and lipids that can lead to programmed cell death. Moreover, most of the current chemotherapeutic compounds suppress cancer cells through generating higher level of ROS and cause significant damage to cancer cells through activation of cell-cycle inhibitors and induction of apoptosis (Zhou et al., 2014).

It has been previously documented that enhanced ROS accumulation plays a crucial role in pro-apoptotic actions of a variety of anticancer carotenoids, including lutein (Kim et al., 2010; Vijay et al., 2018). Therefore, we tested whether lutein could induce ROS accumulation in Hela cells. Cellular ROS levels were determined by cell membrane-permeable fluorescent probe 5-(and-6)-carboxy-2′,7′-dichlorofluorescein diacetate following treatment with lutein for 24 h using both HeLa and MDCK cells. Results showed lower levels of cellular ROS production in normal MDCK cells (1203 ± 210 relative fluorescent unit (RFU)) compared to those in HeLa cells (2166 ± 315 RFU). When cells were treated with 10 μM lutein, intracellular ROS levels were 6215 ± 401 RFU in HeLa cells and 2810 ± 250 RFU in MDCK cells. Lutein significantly increased ROS levels in HeLa cells in a dose-dependent manner (1 μM: 4541 ± 421 RFU, and 10 μM: 6215 ± 401 RFU). Interestingly, treatment with lutein resulted in less ROS levels in MDCK cells (1 μM: 2158 ± 415 RFU, and 10 μM: 2810 ± 250 RFU) than those in HeLa cells. After intracellular ROS was induced by H_2O_2 levels of ROS were 8170 ± 220 RFUL in HeLa cells and 6251 ± 315 RFU in MDCK cells. Interestingly, cellular ROS levels induced by H_2O_2 were decreased by treatment with lutein. These results indicate that lutein has a specific role in cellular ROS production. It acts as an inducer of ROS in cancer cells whereas it is a normalizer in normal cells. Based on available scientific literature, cancer cells are more sensitive to oxidative compounds than normal cells. The generation of a significant amount of ROS has been shown to play a critical role in carotenoid-induced apoptosis of various tumor cells (Kim et al., 2010). Vijay et al. (2018) have also demonstrated that lutein and anticancer drug doxorubicin (DOX) can synergistically enhance cytotoxicity to breast cancer cells by increasing ROS levels.

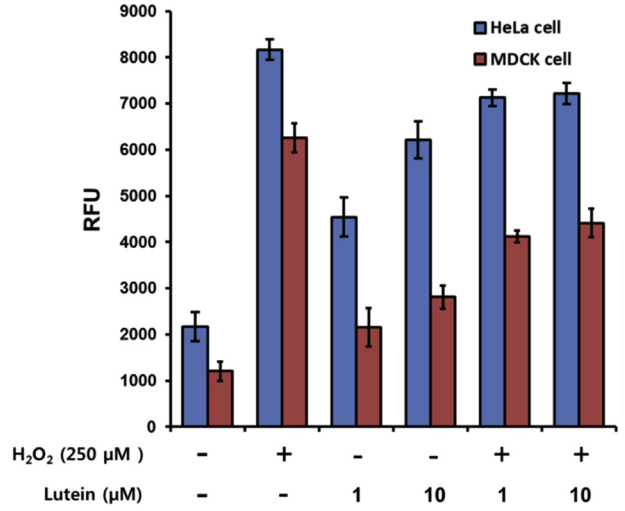

Fig. 3. Effect of lutein on cellular ROS generation. Overproduction of cellular ROS in both HeLa and MDCK cells was induced by treatment with H_2O_2 followed by treatment with lutein (1 and 10 μM) for 24 h. Relative fluorescence of ROS was detected by cell membrane-permeable fluorescent probe carboxy-H2DCFDA. Error bars indicate standard deviation of three independent experiments.

3.4. Lutein mediates regulation of anti-apoptotic and pro-apoptotic family proteins

The rational correlation between anti-apoptotic (Bcl-2) and pro-apoptotic (Bax) mitochondrial proteins can maintain normal mitochondrial functions. Increment of Bax can block Bcl-2 gene expression whereas upregulation of Bcl-2 gene expression can balance Bax gene expression to prolong cell survival (Liu et al., 2014). To confirm lutein-induced apoptosis, we performed qPCR to determine expression levels of apoptotic marker gene in HeLa cells after treatment with lutein. Results showed that expression levels of all apoptosis-related mRNAs studied, including Bcl-2, Bax, tumor protein p53 (p53), and caspase-3, in HeLa cells treated with lutein (1 or 10 μM for 24 h) were significantly changed (Fig. 4). Mitochondrial activity related Bax gene was increased by 1.65 ± 0.21 folds while Bcl-2 gene expression (0.7 ± 0.3 fold) was decreased in HeLa cells treated with 1 μM lutein. Upregulation of p53 and Bax and downregulation of cyclin D1 and Bcl-2 have also been documented in mammary carcinoma MCF-7 cells treated with astaxanthin plus β-carotene and lutein (Sowmya et al., 2017).

Additionally, we able to detect mitochondrial membrane potential loss in the presence of lutein through confocal observation with MitoRed dye on HeLa cells (Fig. 5). Lutein treatment resulted in

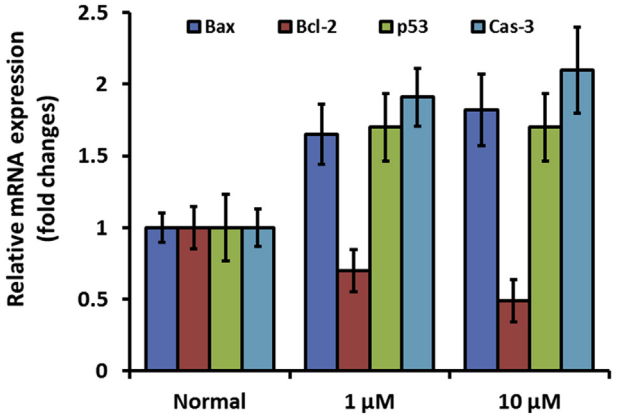

Fig. 4. ROS and cancer-related gene expression induced by lutein. HeLa cells were treated with lutein (1 and 10 μM) for 24 h.

significant reduction of mitochondrial function possible due to loss of balance between Bax and Bcl-2 expression. Furthermore, in the intrinsic apoptotic pathway, increment of Bax can lead to secretion of cytochrome C from mitochondria which induces caspase activation (Zuo et al., 2017).

3.5. Lutein induces activation of caspase-3 and nuclei DNA fragmentation

Caspases, a family of cysteine protease enzymes, are known to play essential roles in programmed cell death. Especially, mitochondria-mediated apoptosis is activated through caspase-3 signaling pathway (Kumar, 2007). Caspase-3 is the vital downstream transductor that is present in most types of cells. It plays a critical role in the starting of apoptosis by cleaving cellular substrates. In the present study, caspase-3 activity was determined in the HeLa cells following lutein treatment. Results showed significantly higher caspase-3 activity in lutein treated HeLa cells (Figs. 3 and 4). Caspase-3 gene expression was increased 1.91 ± 0.2 folds 2.1 ± 0.3 folds after treatment with lutein at 1 μM and 10 μM, respectively, compared to that in untreated cells. Results of immunofluorescence assay also revealed that caspase-3 protein activities were significantly upregulated in lutein treated (1.0 μM) HeLa cells compared to those in nontreated controls (Fig. 5). Despite enhanced activities of caspase-3 protein, nuclei DNAs in nontreated control cells and lutein treated cells were unaffected based on DAPI's sky blue color in both nontreated and lutein-treated HeLa cells (Fig. 5). These observations can be explained by the fact that nuclei DNA fragmentation is one of the last stages of apoptosis in almost all mammalian cells (Elmore, 2007).

In the present study, TUNEL assay was performed to detect nuclei DNA fragmentation. Significant and dose-dependent fragmentation of nuclei DNA was observed in lutein-treated HeLa cells. HeLa cells incubated for 24 h without treatment with carotenoids had 6.7% TUNEL-positive cells. When cells were treated with 1 μM lutein, 72% cells were TUNEL-positive. On the other hand, cells treated with 10 μM of lutein exhibited 97% TUNEL-positive cells (Fig. 6). Significant damage to HeLa nuclei DNA in accordance with activation of caspase-3 suggested that apoptotic actions of lutein were strictly related to the induction of caspase-3 which could induce subsequent cleavage of nuclei DNA. After 12 h of treatment with 10 μM siphonaxanthin, 80.4% TUNEL-positive human leukemia (HL-60) cells were observed (Ganesan et al., 2011). Similarly, fucoxanthin treatment has resulted in nuclei DNA fragmentation in human prostate (PC-3) cancer cells (Kotake-Nara et al., 2005) and Sarcoma 180 (S180) Xenografts-Bearing Mice (Wang et al., 2012). To the best of our knowledge, no previous studies have reported lutein-induced nuclei DNA fragmentation in HeLa cells. In the present investigation, the significant impact of very low concentration (1 μM) of lutein treatment on DNA fragmentation of HeLa cells demonstrates its potential as a bioactive carotenoid. It might have potential as a therapeutic agent to minimize the risk of Human cervical carcinoma. Several naturally derived anticancer drugs have shown to exert the adverse reactions along with their therapeutic potential (Tewari et al., 2019). However, lutein is GRAS for long-term dietary supplementation (Nwachukwu et al., 2016). Thus, the possibilities of adverse drug reactions can be eliminated.

4. Conclusions

In the present study, we provided compelling experimental evidence of lutein-induced dynamic modulation of ROS production in Human cervical carcinoma (Hela) and normal MDCK cell lines. Lutein was found to act as a ROS inducer for HeLa cells while it acted as a normalizer for normal cells. Our results suggest that lutein-induced apoptosis of Hela cells is linked to enhanced ROS generation, loss of mitochondrial membrane potential, and upregulation of Bax and caspase-3-mediated pathway, leading to fragmentation of nuclei DNA. The overall results strongly indicate that lutein could be prospective

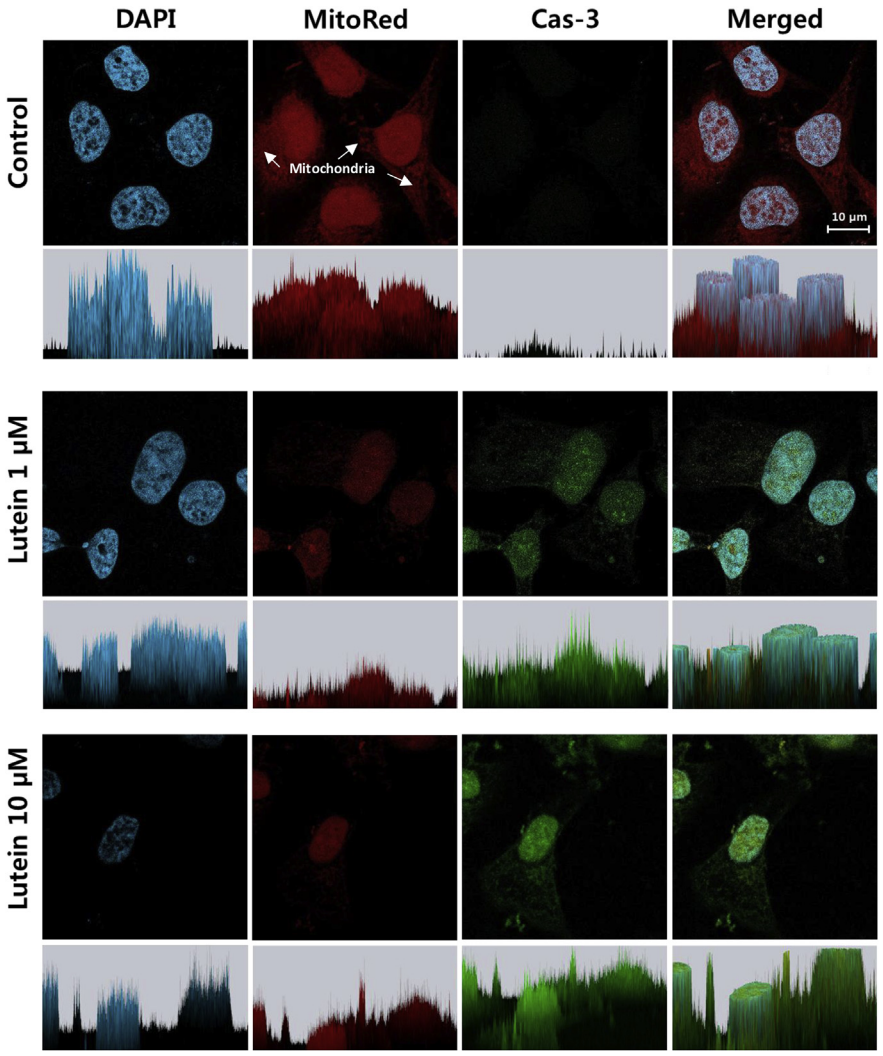

Fig. 5. Confocal observation of the effect of lutein treatment on caspase-3 expression and mitochondrial membrane potential. Lower panel indicates fluorescent intensity. Blue, DAPI (Nuclei); Red, Mitochondrial membrane potential; and Green, Caspase-3 expression. Scale bar, 10 μm. (For interpretation of the references to color in this figure legend, the reader is referred to the Web version of this article.)

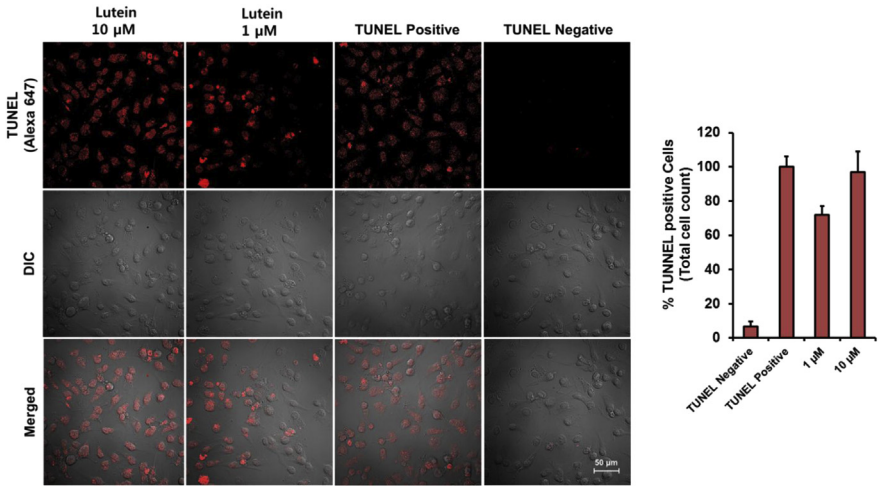

Fig. 6. Lutein induces HeLa cell DNA damage detected by TUNEL assay. HeLa cells were cultured in a confocal dish and maintained for 24 h followed by treatment with lutein (1 and 10 μM) for 24 h. TUNEL assays were then performed. Scale bar, 50 μm.

candidates for chemoprevention and chemotherapeutics of human cervical carcinoma and other chronic diseases. In the future, synergetic effects of lutein with known anticancer drugs could be studied as effective chemotherapy for human cervical carcinoma.

Conflicts of interest

The authors declare that there is no conflict of interest relevant to this study.

Acknowledgment

This paper was supported by KU research professor program of Konkuk University, Seoul, Republic of Korea.

Appendix A. Supplementary data

Supplementary data to this article can be found online at https://doi.org/10.1016/j.fct.2019.02.037.

References

Alvarado-Ramos, K.E., De Leon, L., Fontes, F., Rios-Castillo, I., 2018. Dietary consumption of lutein and zeaxanthin in Panama: a cross-sectional study. Curr Dev Nutr 2. https://doi.org/10.1093/cdn/nzy064.

Bernard, W., 2014. Stewart and Christopher P. Wild.: World Cancer Report, ISBN 978-92-832-0429-9.

Canavan, T.P., Doshi, N.R., 2000. Cervical cancer. Am. Fam. Physician 61, 1369–1376.

Carraher Jr., C.E., 2013. Carraher's Polymer Chemistry, ninth ed. CRC Press, Boca Raton.

Elmore, S., 2007. Apoptosis: a review of programmed cell death. Toxicol. Pathol. 35, 495–516. https://doi.org/10.1080/01926230701320337.

Enkhtaivan, G., Muthuraman, P., Kim, D.H., 2017. Inhibitory effect of 2,4-dichlorophenoxyacetic acid on ROS, autophagy formation, and mRNA replication for influenza virus infection. J. Mol. Recogn. 30. https://doi.org/10.1002/jmr.2616.

Ganesan, P., Noda, K., Manabe, Y., Ohkubo, T., Tanaka, Y., Maoka, T., Sugawara, T., Hirata, T., 2011. Siphonaxanthin, a marine carotenoid from green algae, effectively induces apoptosis in human leukemia (HL-60) cells. Biochim. Biophys. Acta 1810, 497–503. https://doi.org/10.1016/j.bbagen.2011.02.008.

Gansukh, E., Kazibwe, Z., Pandurangan, M., Judy, G., Kim, D.H., 2016. Probing the impact of quercetin-7-O-glucoside on influenza virus replication influence. Phytomedicine 23, 958–967. https://doi.org/10.1016/j.phymed.2016.06.001.

Henderson, R.K., Jiménez-González, C., Constable, D.J.C., Alston, S.R., Inglis, G.G.A., Fisher, G., Sherwood, J., Binks, S.P., Curzons, A.D., 2011. Expanding GSK's solvent selection guide – embedding sustainability into solvent selection starting at medicinal chemistry. Green Chem. 13, 854–862. https://doi.org/10.1039/C0GC00918K.

Hojnik, M., Škerget, M., Knez, Z., 2008. Extraction of lutein from marigold flower petals – experimental kinetics and modelling. LWT - Food Sci. Technol. (Lebensmittel-Wissenschaft -Technol.) 41, 2008–2016. https://doi.org/10.1016/j.lwt.2007.11.017.

Hurst, W., 2008. Methods of Analysis for Functional Foods and Nutraceuticals. CRC Press, Boca Raton. https://doi.org/10.1201/9781420007152.

Kim, D.-E., Shang, X., Assefa, A.D., Keum, Y.-S., Saini, R.K., 2018. Metabolite profiling of green, green/red, and red lettuce cultivars: variation in health beneficial compounds and antioxidant potential. Food Res. Int. 105, 361–370. https://doi.org/10.1016/j.foodres.2017.11.028.

Kim, K.-N., Heo, S.-J., Kang, S.-M., Ahn, G., Jeon, Y.-J., 2010. Fucoxanthin induces apoptosis in human leukemia HL-60 cells through a ROS-mediated Bcl-xL pathway. Toxicol. Vitro 24, 1648–1654. https://doi.org/10.1016/j.tiv.2010.05.023.

Kotake-Nara, E., Asai, A., Nagao, A., 2005. Neoxanthin and fucoxanthin induce apoptosis in PC-3 human prostate cancer cells. Cancer Lett. 220, 75–84. https://doi.org/10.1016/j.canlet.2004.07.048.

Kotake-Nara, E., Kushiro, M., Zhang, H., Sugawara, T., Miyashita, K., Nagao, A., 2001. Carotenoids affect proliferation of human prostate cancer cells. J. Nutr. 131, 3303–3306.

Krinsky, N.I., Johnson, E.J., 2005. Carotenoid actions and their relation to health and disease. Mol. Aspect. Med. 26, 459–516. https://doi.org/10.1016/j.mam.2005.10.001.

Kumar, S., 2007. Caspase function in programmed cell death. Cell Death Differ. 14, 32–43. https://doi.org/10.1038/sj.cdd.4402060.

Lakshminarayana, R., Sathish, U.V., Dharmesh, S.M., Baskaran, V., 2010. Antioxidant and cytotoxic effect of oxidized lutein in human cervical carcinoma cells (HeLa). Food Chem. Toxicol. 48, 1811–1816. https://doi.org/10.1016/j.fct.2010.04.011.

Liu, J., Yao, Y., Ding, H., Chen, R., 2014. Oxymatrine triggers apoptosis by regulating Bcl-2 family proteins and activating caspase-3/caspase-9 pathway in human leukemia HL-60 cells. Tumor Biol. 35, 5409–5415. https://doi.org/10.1007/s13277-014-1705-7.

Niranjana, R., Gayathri, R., Nimish Mol, S., Sugawara, T., Hirata, T., Miyashita, K., Ganesan, P., 2015. Carotenoids modulate the hallmarks of cancer cells. Journal of Functional Foods, Natural Antioxidants 18, 968–985. https://doi.org/10.1016/j.jff.2014.10.017.

Nupur, L.N.U., Vats, A., Dhanda, S.K., Raghava, G.P.S., Pinnaka, A.K., Kumar, A., 2016. ProCarDB: a database of bacterial carotenoids. BMC Microbiol. 16, 96. https://doi.org/10.1186/s12866-016-0715-6.

Nwachukwu, I.D., Udenigwe, C.C., Aluko, R.E., 2016. Lutein and zeaxanthin: production technology, bioavailability, mechanisms of action, visual function, and health claim status. Trends Food Sci. Technol. 49, 74–84. https://doi.org/10.1016/j.tifs.2015.12.005.

Pandurangan, M., Enkhtaivan, G., Kim, D.H., 2016. Therapeutic efficacy of natural dipeptide carnosine against human cervical carcinoma cells. J. Mol. Recogn. 29, 426–435. https://doi.org/10.1002/jmr.2541.

Pham-Huy, L.A., He, H., Pham-Huy, C., 2008. Free radicals, antioxidants in disease and health. Int. J. Biomed. Sci. 4, 89–96.

Rodriguez-Amaya, D.B., 2001. A Guide to Carotenoid Analysis in Foods. Ilsi Press, Washington, D. C.

Saini, R.K., Moon, S.H., Gansukh, E., Keum, Y.-S., 2018. An efficient one-step scheme for the purification of major xanthophyll carotenoids from lettuce, and assessment of their comparative anticancer potential. Food Chem. 266, 56–65. https://doi.org/10.1016/j.foodchem.2018.05.104.

Sowmya, P.R.-R., Arathi, B.P., Vijay, K., Baskaran, V., Lakshminarayana, R., 2017. Astaxanthin from shrimp efficiently modulates oxidative stress and allied cell death progression in MCF-7 cells treated synergistically with β-carotene and lutein from greens. Food Chem. Toxicol. 106, 58–69. https://doi.org/10.1016/j.fct.2017.05.024.

Tewari, D., Rawat, P., Singh, P.K., 2019. Adverse drug reactions of anticancer drugs derived from natural sources. Food Chem. Toxicol. 123, 522–535. https://doi.org/10.1016/j.fct.2018.11.041.

van Breemen, R.B., Dong, L., Pajkovic, N.D., 2012. Atmospheric pressure chemical ionization tandem mass spectrometry of carotenoids. Int. J. Mass Spectrom. 312, 163–172. https://doi.org/10.1016/j.ijms.2011.07.030.

Vechpanich, J., Shotipruk, A., 2010. Recovery of free lutein from *Tagetes erecta*: determination of suitable saponification and crystallization conditions. Separ. Sci. Technol. 46, 265–271. https://doi.org/10.1080/01496395.2010.506904.

Vichai, V., Kirtikara, K., 2006. Sulforhodamine B colorimetric assay for cytotoxicity screening. Nat. Protoc. 1, 1112–1116. https://doi.org/10.1038/nprot.2006.179.

Vijay, K., Sowmya, P.R.-R., Arathi, B.P., Shilpa, S., Shwetha, H.J., Raju, M., Baskaran, V., Lakshminarayana, R., 2018. Low-dose doxorubicin with carotenoids selectively alters redox status and upregulates oxidative stress-mediated apoptosis in breast cancer cells. Food Chem. Toxicol. 118, 675–690. https://doi.org/10.1016/j.fct.2018.06.027.

Wang, H., Naghavi, M., Allen, C., Barber, R.M., Bhutta, Z.A., Carter, A., CDasey, D.C., G.B., Murray, C.J.L., et al., 2016. Global, regional, and national life expectancy, all-cause mortality, and cause-specific mortality for 249 causes of death, 1980–2015: a systematic analysis for the Global Burden of Disease Study 2015. Lancet 388, 1459–1544. https://doi.org/10.1016/S0140-6736(16)31012-1.

Wang, J., Chen, S., Xu, S., Yu, X., Ma, D., Hu, X., Cao, X., 2012. In Vivo induction of apoptosis by fucoxanthin, a marine carotenoid, associated with down-regulating STAT3/EGFR signaling in sarcoma 180 (S180) xenografts-bearing mice. Mar. Drugs 10, 2055–2068. https://doi.org/10.3390/md10092055.

Widomska, J., Subczynski, W.K., 2014. Why has nature chosen lutein and zeaxanthin to protect the retina? J. Clin. Exp. Ophthalmol. 5, 326. https://doi.org/10.4172/2155-9570.1000326.

Zhou, D., Shao, L., Spitz, D.R., 2014. Reactive oxygen species in normal and tumor stem cells. Adv. Cancer Res. 122, 1–67. https://doi.org/10.1016/B978-0-12-420117-0.00001-3.

Zuo, W., Yan, F., Zhang, B., Li, J., Mei, D., 2017. Advances in the studies of ginkgo biloba leaves extract on aging-related diseases. Aging Dis 8, 812–826. https://doi.org/10.14336/AD.2017.0615.